A New Control Architecture for Physical Human-Robot Interaction Based on Haptic Communication

by

Yusuf Aydın

A Thesis Submitted to the
Graduate School of Engineering
in Partial Fulfillment of the Requirements for
the Degree of

Master of Science
in
Mechanical Engineering

Koc University

September 2013

Koc University

Graduate School of Sciences and Engineering

This is to certify that I have examined this copy of a master's thesis by

Yusuf Aydın

and have found that it is complete and satisfactory in all respects,

and that any and all revisions required by the final

examining committee have been made.

Committee Members:

____

Cagatay Basdogan, Assoc. Prof. Dr. (Advisor)

____

Hakan Temeltas, Prof. Dr.

____

Volkan Patoglu, Assoc. Prof. Dr.

Date: 18.09.2013

to my beloved family…

ABSTRACT

In the near future, humans and robots are expected to perform collaborative tasks involving physical interaction in various different environments such as homes, hospitals, and factories. One important research topic in physical Human-Robot Interaction (pHRI) is to develop tacit and natural haptic communication between the partners. Although there are already several studies in the area of Human-Robot Interaction, the number of studies investigating the physical interaction between the partners and in particular the haptic communication are limited and the interaction in such systems is still artificial when compared to natural human-human collaboration. For example, when two people collaborate to transport a table, they can intuitively sense each other's intention and decide on load sharing and role allocation based on the state of the table and the forces transmitted to each other. Moreover, they can resolve the conflicts occurring in constrained environments based on the force interaction again. Although the tasks involving physical interaction such as the table transportation can be planned and executed naturally and intuitively by two humans, there are unfortunately no robots in the market that can collaborate and perform the same tasks with us. In this thesis, we propose a new controller for the robotic partner that is designed to a) detect the intentions of the human operator through haptic channel using a fuzzy controller b) adjust its contribution to the task via a variable impedance controller and c) resolve the conflicts during the task execution by controlling the internal forces.

ÖZET

Yakın gelecekte ev, hastane, fabrika gibi çeşitli ortamlarda, insanların ve robotların birlikte fiziksel işbirliğine dayalı işler yapması beklenmektedir. Fiziksel insan-robot etkileşimi alanındaki önemli araştırma konularından birisi, insanlar ve robotlar arasında dokunma duyusu odaklı iletişimi doğal şekilde sağlayabilecek sistemler geliştirmektir. İnsan-robot fiziksel etkileşimi üzerine araştırmalar yapılmıştır, fakat bu çalışmalar hem sınırlı sayıdadır hem de bu sistemlerdeki etkileşim insan-insan etkileşimine kıyasla hala yapay kalmaktadır. Örneğin, iki insan bir masayı taşırken sezgisel olarak birbirlerinin ne yapmak istediklerini, amaçlarını algılayıp, bu algılara, masanın durumuna ve birbirlerine masa aracılığı ile transfer ettikleri kuvvet bilgilerine dayanarak yük paylaşımını ve rol dağılımını rahatlıkla yapabilirler. Ayrıca, kısıtlı ortamlarda, aralarında oluşan anlaşmazlıkları yine kuvvet etkileşimleri üzerinden çözümlerler. İki insan, fiziksel etkileşim gerektiren işleri, sezgilerini kullanarak hem planlayabilip hem de rahatlıkla yerine getirebilmesine rağmen, maalesef piyasada aynı işleri bizlerle beraber, benzer şekillerde yapabilecek robotlar bulunmamaktadır. Bu tez çalışmasında, fiziksel etkileşim gerektiren bir görevi, bir insan ile ortaklaşa çalışarak yerine getirebilecek bir robot için yeni bir kontrol yapısı öneriyoruz. Bu kontrol sistemi a) görevin yapılması sırasında insanın anlık niyetini, kuvvet etkileşimlerini kullanarak, bulanık kontrol mantığı ile tespit etmeyi, b) robotun göreve olan katkısını empedansı ayarlanabilir bir kontrolcü kullanarak belirlemeyi ve c) insan ile robot arasındaki oluşan anlaşmazlıkları, birbirlerine zıt, iç kuvvetleri minimize ederek çözümlemeyi, amaçlamaktadır.

ACKNOWLEDGEMENTS

I would like to express my sincere gratitude to my thesis supervisor Assoc. Prof. Cagatay Basdogan for his support, valuable criticism and guidance, and endless patience, motivation, encouragement and enthusiasm throughout my study. He supported me not only with our research study but also with my decisions about my professional and social life. His work and dedication to the research is always amazed me and I will never forget and hopefully continue to our worthwhile research meetings. I would like to also express my deepest gratitude to Prof. Hakan Temeltas and Assoc. Prof. Volkan Patoglu especially for their precious time that they spent during my thesis defense and for their valuable criticism, suggestions and guidance for my thesis.

I would like to thank to Ayse Kucukyilmaz, Ph.D. She is and always will be one of the great people that I am happy to meet and know. Her support and advice regarding to my career and despite the strong disagreements, arguments and debates, leading to that we even get angry with each other, I will never forget them. At each disagreement, or at each advice, I learnt a significant lesson regardless of whether I am right or wrong.

I would like to thank Arda Aytekin. I don’t know how to start to tell about him. He is always the person who helped everybody around him. If his help, motivations, and interventions weren’t occurred, probably, today I wouldn’t be neither defending nor writing my thesis. All my depressed times, related with my research or my problems related to my life, he was always there to talk to. Even he was graduated and went to abroad for his Ph.D., he was still dealing with my ridiculous problems. Thank you, Arda.

My dear friend for 11 years now, my flat-mate, my colleague, Gökhan Nadar, I don’t know how to thank him. He was always there for me and I am sure he will always be. His especially moral support in every problem that I encountered will never be forgotten. Also I will never forget the times that we studied to solve unbearable engineering problems together. He is the person who took me from the deep of the ocean and brought me back to the surface in my the most desperate moments.

I would like to thank to Çağrı Yeşil. He was always a big brother to me since I met him. I will never forget what he taught me. And I am truly grateful to him. I will never forget the walk with Kübra Gültekin on an autumn evening. The moral support that she gave me was unforgettable. I would like to thank Pelin Dogan, Nilüfer Karaagac and Bora Karasulu for their support and friendship. Especially for the last year of my study, I will always remember Gökçenur Bilgin and Gökçe Bal and their cute little home. I would like to thank Hatice and İsmail Menekşe for their kindness, warm ambient and delicious food they cooked. I would like to thank Nasser Arghavani and Cigil Ece Madan for their help and support in my studies. It was a privilege to know and work with them as well as Mohammad Ansarin, Atakan Arasan, Mehmet Ayyildiz, Buket Baylan, Soner Cinoglu, Enes Selman Ege, Senem Ezgi Emgin, Yasemin Vardar, Berkay Yarpuzlu, Mustafa Yılmaz.

Whenever I recall the memories of my M.Sc. study times, I will always remember the name Ayca Bal, who was a great person to know, to see, to talk to, and to dance with. I cannot imagine my M.Sc. period without her. And, she most certainly deserves the most gratitude that is possible for my last two years. I will never forget about her tactful contribution, motivation and support that she gave.

I would like to thank my entire family and especially my father, my mother and my elder and little brothers. They always believed in me and supported me through my studies and my life. Sometimes they doubted about what I am going to do but they always helped me to decide. When I had any problems in my life to solve and any happines to share, I hope and I am sure that they will still be there for me.

Finally, I would like to express my gratitude to TUBITAK-BIDEB for financially supporting me through my M.Sc. studies.

TABLE OF CONTENTS

LIST OF TABLES

LIST OF FIGURES

Chapter 1

INTRODUCTION

The controller proposed in this thesis is designed for a robot collaborating with a human partner and handling long and bulky objects in different environments. In our architecture, the human partner always leads the task and the robot simply complies with his/her intentions. These intentions are conveyed to the robot through haptic (force) channel. Hence, we assume that the robot infers to the human partner's intentions through the sensors attached to its body and/or in the environment to execute the task successfully with the human partner. For example, in a home setting, a robot may collaborate with a human user to assemble or move furniture. In a hospital, a robot may work with a staff to transport a patient lying on a wheeled bed. In a factory, a robot and a worker may install a windshield on a car together. In all of these scenarios, the task requires more than one person to accomplish since the object being manipulated (furniture, bed, windshield) is long, bulky, and heavy for a single person to handle. Although there are already several studies available on Human-Robot Interaction (HRI) in the literature, the number of studies investigating the physical Human-Robot Interaction (pHRI) and in particular the haptic communication between the partners are limited and the interaction in such systems is still artificial when compared to natural human-human collaboration.

To make human-robot collaboration more natural, we need robots that can anticipate the intentions of the human partner and comply with those intentions smoothly during the execution of a collaborative task. Obviously, the intention is a state of mind, which cannot be measured directly. However, we know that humans are good at recognizing each others' intentions during a collaborative task even without a verbal communication. For instance, Stefanov et al. (2009) proposed executor and conductor roles for human-human haptic interaction. The executor mainly contributes to the execution of the task on the other hand the conductor takes the decision and controls the motion, expressing his/her intentions via haptic signals so that the executor can perform these actions. This system is especially interesting in a sense that the parties are required to communicate only through the haptic channel, i.e. the conductor is assumed to express his/her intention by applying larger forces.

Although the collaborating human partners may use other means of communication such as voice commands and gestures to convey their intentions while transporting a table, the haptic channel is more direct and personal than those when there is a physical interaction. Also, when a human partner performs the same task with a robot cooperatively, it would be necessary to tell the robot the intended direction and speed of movement continuously, which would be tiring for the human operator. For example, while transporting a table, the human operator must explicitly express his/her intention of movement to the robot using words such as "Left", "Right", "Clockwise", "Counterclockwise" and explicitly adjust the speed of the task using the words such as "Slow", "Fast", "Continue", "Stop". However, if the robot is equipped with a force sensor and can track the table pose using its stereo cameras, the above information can be intuitively conveyed through the haptic channel. Here, the intended movement can be conveyed to the robot via the direction of the force applied to the table by the human operator while the force magnitude helps with the speed of the movement. In de Carli et al. (2009), the robot assumes that human operator intends to change the direction of motion when he/she exceeds a predetermined force threshold in that direction. Duchaine and Gosseline (2007) utilized the derivative of the force applied by the human operator and the velocity of the manipulated object to predict whether the human operator intends to accelerate or decelerate the object. Wojtara et al. (2009) developed a robotic assistant for collaborative positioning of windshields during car manufacturing. They separated the degrees of freedom of the task and weighted the robot's contribution to each degree of freedom based on the forces applied by the human operator. Dumora et al. (2013) decomposed the manipulation task into a sequence of elementary motions (rotations and translations) and human intention is detected by analyzing the forces applied by the human operator.

Following the intention recognition, the collaborating human partners successfully adjust their forces to adapt not only to the requirements of the task but also to each other's needs (Dourish and Bellotti, 1992). Again, in the table transportation task, if one of the human partners pushes the table hard to speed up, the other can stiffen his/her muscles to comply with this movement or to slow it down. This adjustment is possible because, we, human beings, can adjust our arm impedance by adjusting the muscle contraction level. This is so-called "impedance control" has been studied extensively by many researchers in robotics literature (Hogan, 1985). Ikeura et al. (1994) investigated the dynamical characteristics of human arm in a cooperation task performed by two humans and they showed that human arm dynamics can be expressed by impedance control. Later (Ikeura et al., 2002), they designed an impedance controller for a robotic assistant using the impedance values obtained from human-human experiments. Takubo et al. (2002) implemented virtual constraints with an impedance controller to constraint the movements of the robot arm during a pHRI task. In their approach, a robotic partner renders a virtual nonholonomic constraint –namely a virtual wheel– that prohibits sideway slipping motion. This approach however, inhibits maneuvering of bulky objects in narrow passages. Mörtl et al. (2012) combined an impedance controller with a role exchange mechanism suggested in

Oguz et al. (2010) to adjust the contribution of the robotic partner dynamically during a pHRI task.

More recently, variable impedance control has been proposed to control physical interaction taking place between a human operator and a robot. The fundamental idea here is to change the impedance parameters of the robotic controller adaptively according to the requirements of the task and the needs of the human operator. Ikeura et al. (2002) suggested that the dynamical characteristics of a human arm can be regarded as an optimal damper and by varying the impedance damping of a robot arm based on the human impedance characteristics, smooth manipulation trajectories can be obtained during a pHRI task. Duchaine and Gosseline (2007) implemented a variable impedance control scheme for human robot cooperation. They utilized the derivative of the force applied by the human operator and the velocity of the manipulated object to estimate the intention of the human operator and alter the damping coefficient of the impedance controller accordingly.

In this thesis, we propose a new control architecture for pHRI involving haptic communication. We consider the following constraints while developing this control architecture:

- The task involves handling a large and bulky object in a collaborative manner. Neither the human operator nor the robot can do the task alone.
- The task involves physical interaction between the human operator and the robot all the time.
- The human operator always leads the task, the robot is just a follower and does not take initiatives during the task execution.
- The communication between the human operator and the robot is through the haptic channel only and it is not feasible to measure the force applied by the human operator.
- The robot does not know the task trajectory in advance.

This architecture has three major components: 1) an intention estimator, which detects the intentions of the human operator through haptic channel using a fuzzy controller, 2) a variable impedance controller, which adjusts the contribution of the robot to the task based on the intentions of the human partner, and 3) an internal force compensator, which resolves the conflicts during the task execution by controlling the internal forces. We are not aware of any earlier approach that integrates these three components together in a coherent manner. Although an intention estimator together with a variable impedance controller has been suggested for pHRI in the past (Duchaine and Gosseline, 2007), the robot's impedance has been altered using a simple rule based algorithm. Moreover, how fast the robot should adapt to the intentions of the human operator has not been considered for setting the gains of the variable impedance controller. We propose to use a fuzzy controller to estimate the human intention using a continuous function, which provides smooth transitions. Also, we suggest a method to include the how swift the robot should react to the human intention while setting the gains. Finally, the "internal force" has been utilized as a measure of conflict in earlier pHRI studies (Ikeura et al., 1994; Groten et al., 2009; Stefanov et al., 2009; Kucukyilmaz, 2013; Mörtl et al., 2012) and the internal force controller has been utilized to manipulate an object collaboratively using multiple robots in earlier robotic studies (Seraji and Colbaugh, 1997; Jung et al. 2004; Stanistic and Fernandez, 2012), but, to our knowledge, it has not been used at all in earlier pHRI studies to resolve force conflicts between a human operator and a robot.

Chapter 2

CONTROL ARCHITECTURE

In order to demonstrate the proposed control architecture, we further simplify the table transportation task and make it one dimensional. In other words, we assume that the human operator and the robot translate the table between two stations along a straight path only and the table is treated as a point mass.

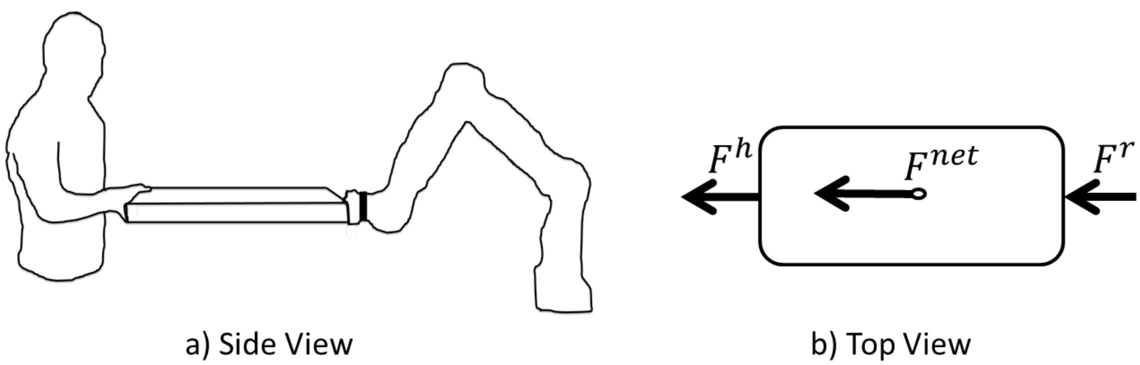

Figure 2.1. The table transportation task investigated in this thesis.

In our architecture, the robot does not know the final destination; hence no positional trajectory is specified for the robot. The task is initiated by the human operator. The center velocity of the table is measured using cameras and/or some other sensors such as accelerometers. The force applied by the robot to the table is measured by a force sensor at the wrist of the robot. Based on these measurements, the current states of the table and the force applied by the human operator are estimated via a Kalman observer.

$$\boldsymbol{x} = \begin{bmatrix} x \\ v \end{bmatrix} \tag{2.1}$$

$$\boldsymbol{A}_c = \begin{bmatrix} 0 & 1 \\ 0 & 0 \end{bmatrix} \tag{2.2}$$

$$\boldsymbol{B}_c = \begin{bmatrix} 0 \\ 1/M \end{bmatrix} \tag{2.3}$$

$$\boldsymbol{C}_c = \begin{bmatrix} 0 & 1 \end{bmatrix} \tag{2.4}$$

$$\dot{\boldsymbol{x}} = \boldsymbol{A}_c \begin{bmatrix} x \\ v \end{bmatrix} + \boldsymbol{B}_c \left[\overbrace{F^r + F^h}^{u} \right] \tag{2.5}$$

$$y = C_c \boldsymbol{x} \tag{2.6}$$

Here, $\boldsymbol{x}$ represents the continuous states of the table (i.e. plant), u is the sum of the forces applied by the human operator and the robot to the table. The mass, M, of the table is 44 kg. The matrices $\boldsymbol{A}_c$, $\boldsymbol{B}_c$ and $\boldsymbol{C}_c$ are the continuous time state, input, and the output matrices of the plant, respectively. $F^r$and F^h are the force applied by the robot and the human operator, respectively.

We use a Kalman observer to estimate the force applied by the human during the task execution since it cannot be measured directly during the task execution (i.e. it is not feasible to attach a force sensor to the human operator or the object being manipulated in a real-life scenario). For this purpose, we augment the state vector of the table to include the human force as a disturbance and re-define it in discrete domain as

$$\boldsymbol{X_k} = \begin{bmatrix} x_k \\ v_k \\ F_k^h \end{bmatrix} \tag{2.7}$$

Since we will estimate the human force like a disturbance and we need a dynamic model for disturbance to estimate it, we assume that the disturbance (human force) is a sequence of perturbed piecewise constant signals, expressed as

$$F_{k+1}^{h} = F_{k}^{h} + w_{k}^{w} \tag{2.8}$$

Then, the state space equations of the table can be re-written in discrete domain to use in Kalman observer as

$$\boldsymbol{X}_{k+1} = \boldsymbol{A}\boldsymbol{X}_{k} + \boldsymbol{B}F_{k}^{r} + \mathbf{W}w_{k}^{w} \tag{2.9}$$

$$y_{k} = \boldsymbol{C}\boldsymbol{X}_{k} + w_{k}^{v} \tag{2.10}$$

$$\boldsymbol{X}_{k+1} = \begin{bmatrix} \boldsymbol{A}_{d} & \boldsymbol{B}_{d} \\ \mathbf{0}_{1x2} & 1 \end{bmatrix} \boldsymbol{X}_{\boldsymbol{k}} + \begin{bmatrix} \boldsymbol{B}_{d} \\ 0 \end{bmatrix} F^{r} + \begin{bmatrix} \boldsymbol{W}_{d} \\ 1 \end{bmatrix} w_{k}^{w} \tag{2.11}$$

$$y_{k} = [\boldsymbol{C}_{d} \quad 0]\boldsymbol{X}_{k} + \ w_{k}^{v} \tag{2.12}$$

$$\boldsymbol{A}_{d} = \begin{bmatrix} 1 & 0.01 \\ 0 & 1 \end{bmatrix} \tag{2.13}$$

$$\boldsymbol{B}_{d} = 1x10^{-3}[0.0011 \quad 0.2273]^{T} \tag{2.14}$$

$$\boldsymbol{C}_{d} = [0 \quad 1] \tag{2.15}$$

Here, $\boldsymbol{X}_{\boldsymbol{k}}$ represents the augmented states of the plant, $F^{r}$is the force applied by the robot (i.e. input to the plant), $w_{k}^{w}$is the Gaussian state noise, y_{k} is the output, and w_{k}^{v} is the Gaussian measurement noise at time instance *k*. The matrices $\boldsymbol{A}$, $\boldsymbol{B}$ and $\boldsymbol{C}$ are the state, input, and the output matrices of the plant, respectively. $\boldsymbol{W}_{d}$ determines how the non-augmented states of the table are affected by the state noise and the states including human force are assumed to be affected by the Gaussian state noise (see the $\boldsymbol{W}$ vector in Equation (2.11)).

Kalman Observer is a tool to observe the states of a dynamic system which may or may not be measurable. Kalman observer makes a prediction of the current state based on the previous states and the input using the system model. Then according to the current output measurement and the Kalman gain, Kalman Observer makes the appropriate correction to the current state estimates.

$$\widehat{\boldsymbol{X}}_{k|k-1} = \boldsymbol{A}\widehat{\boldsymbol{X}}_{k-1|k-1} + \boldsymbol{B}u_{k-1} \tag{2.16}$$

$$\hat{y}_{k|k-1} = \boldsymbol{C}\widehat{\boldsymbol{X}}_{k|k-1} \tag{2.17}$$

$$\widehat{\boldsymbol{X}}_{k|k} = \widehat{\boldsymbol{X}}_{k|k-1} + \boldsymbol{K}(y_k - \hat{y}_{k|k-1}) \tag{2.18}$$

Next, we design the Linear Quadratic Estimator (LQE) based on the standard Kalman filter implementation as follows:

$$\boldsymbol{P}_{k|k-1} = \boldsymbol{A}\boldsymbol{P}_{k-1|k-1}\boldsymbol{A}^T + \boldsymbol{W}R_w\boldsymbol{W}^T \tag{2.19}$$

$$\boldsymbol{K} = \boldsymbol{P}_{k|k-1}\boldsymbol{A}^T(\boldsymbol{A}\boldsymbol{P}_{k|k-1}\boldsymbol{A}^T + R_v)^{-1} \tag{2.20}$$

$$\boldsymbol{P}_{k|k} = (\boldsymbol{I} - \boldsymbol{K}\boldsymbol{A})\boldsymbol{P}_{k|k-1} \tag{2.21}$$

$$\widehat{\boldsymbol{X}}_{k|k} = \underbrace{(\boldsymbol{I} - \boldsymbol{K}\boldsymbol{C})\boldsymbol{A}}_{\boldsymbol{K_1}}\widehat{\boldsymbol{X}}_{k-1|k-1} + \underbrace{(\boldsymbol{I} - \boldsymbol{K}\boldsymbol{C})\boldsymbol{B}}_{\boldsymbol{K_2}}F^r_{k-1} + \boldsymbol{K}\boldsymbol{y}_k \tag{2.22}$$

Here, $\boldsymbol{P}_{i|j}$ and $\widehat{\boldsymbol{X}}_{i|j}$ represent the variance of the estimation error and the estimated states at time instance *i* based on the information available at time instance *j*, respectively, and $\boldsymbol{I}$ is the identity matrix of appropriate size. Also, R_w is the variance of the Gaussian state noise and R_v is the variance of the Gaussian measurement noise, which is assumed to be $R_v = 1$

mm in our system. The ratio of R_w / R_v represents the relative importance of modeling uncertainty to the measurement uncertainty and selected as 100. The static (i.e. steady state) observer gain $\boldsymbol{K}$, and hence the static gains $\boldsymbol{K_1}$and $\boldsymbol{K_2}$ are obtained offline by iteratively solving Equations (2.19) through (2.21) until $\boldsymbol{P}_{k|k}$ converges. Note that the observer gain is determined based on $\boldsymbol{W}$ vector and this vector determines how the estimated force applied by the human was perturbed by the state noise. Since the amount of the state noise is estimated from the error between the predicted and measured values of the output (i.e. velocity) and since it is clear that the human force is perturbed by this state noise, at each time depending on the $\boldsymbol{K}$ (through $\boldsymbol{W}$**),** the estimated human force is updated.

In order to regulate the force applied by the robot to the table, the controller needs to know the desired trajectory of the table. However, for a pHRI task, it is not practical to assume that the robot knows the desired trajectory of the manipulated object in advance. For this reason, we predict the next state of the table at each time step using a simple kinematics predictor based on the previous states. For this purpose, we utilize the Kalman observer equations at the prediction stage based on the non-augmented discrete states.

$$\hat{\boldsymbol{x}}_{k+1|k} = \boldsymbol{A}_d \hat{x}_{k|k} + \boldsymbol{B}_d u_k \tag{2.23}$$

$$\hat{\boldsymbol{x}}_{k+1|k} = \boldsymbol{A}_d \left[\hat{x}_{k|k-1} + \boldsymbol{K}_{2x1} \left(y_k - \hat{y}_{k|k-1} \right) \right] + \boldsymbol{B}_d u_k \tag{2.24}$$

$$\begin{aligned} \hat{\boldsymbol{x}}_{k+1|k} = \boldsymbol{A}_d \left[\hat{x}_{k|k-1} + \ \boldsymbol{K}_{2x1} \left(y_k - \boldsymbol{C} \hat{x}_{k|k-1} \right) \right] \\ + \boldsymbol{B}_d u_k \end{aligned} \tag{2.25}$$

$$\begin{aligned} \hat{\boldsymbol{x}}_{k+1|k} = \boldsymbol{A}_d \Big[& \boldsymbol{A}_d \hat{\boldsymbol{x}}_{k-1|k-1} + \boldsymbol{B}_d u_{k-1} \\ & + \boldsymbol{K}_{2x1} \Big(y_k - \boldsymbol{C} \big(\boldsymbol{A}_d \hat{\boldsymbol{x}}_{k-1|k-1} + \boldsymbol{B}_d u_{k-1} \big) \Big) \Big] + \boldsymbol{B}_d u_k \end{aligned} \tag{2.26}$$

$$\hat{\boldsymbol{x}}_{k+1|k} = \overbrace{(\boldsymbol{A}_d - \boldsymbol{A}_d\boldsymbol{K}_{2x1}\boldsymbol{C})\boldsymbol{A}_d}^{\boldsymbol{K}_1^p}\,\hat{x}_{k-1|k-1} + \overbrace{\boldsymbol{A}_d\boldsymbol{K}_{2x1}}^{\boldsymbol{K}_2^p}\,y_k + \underbrace{(\boldsymbol{A}_d - \boldsymbol{A}_d\boldsymbol{K}_{2x1}\boldsymbol{C})\boldsymbol{B}_d}_{\boldsymbol{K}_3^p}\,u_{k-1} + \boldsymbol{B}_d u_k \tag{2.27}$$

We insert $u_{k-1} = F^r_{k-1} + \hat{F}^h_{k-1|k-1}$ (note that $\hat{F}^h_{k-1|k-1}$ is already estimated in $\hat{\boldsymbol{X}}_{k|k}$) and $u_k = F^r_k + \hat{F}^h_{k-1|k-1}$ (since we don't know $\hat{F}^h_{k|k}$ yet) into the Equation (2.27).

$$\hat{\boldsymbol{x}}_{k+1|k} = \boldsymbol{K_1^p}\hat{x}_{k-1|k-1} + \boldsymbol{K_2^p}y_k + \boldsymbol{K_3^p}\left(F^r_{k-1} + \hat{F}^h_{k-1|k-1}\right) + \boldsymbol{B}_d(F^r_k + \hat{F}^h_{k-1|k-1}) \tag{2.28}$$

where $\boldsymbol{K_1^p}, \boldsymbol{K_2^p}, \boldsymbol{K_3^p}$ and $\boldsymbol{B}_d$ are the state, output, previous input and current input prediction matrices.

Once the next state of the table is predicted based on the previous one, the force applied by the robot to the table (F^r_{des}) is calculated by an impedance controller in our approach. An impedance control utilizes a single control law which attempts to regulate both position and force by specifying a dynamic relationship between them. This relationship is chosen to be a second-order linear impedance because such systems are well understood and simple to control. A standard impedance control law is shown in Equation (2.29), where m, b, k are the controller impedance mass, damping and stiffness, x_{des} and v_{des} are the desired position and velocity of the end-effector, x, v, a are the actual position, velocity, and accelaration of the end-effector, K_p and K_i are the proportional and integral motion feedback gains, respectively.

$$F^r_{des} = ma + bv + kx + K_p(v_{des} - v) + K_i(x_{des} - x) \tag{2.29}$$

If we neglect the impedance mass and stiffness (m = 0, k = 0) and define

$$e = (v_{des} - v) \tag{2.30}$$

$$\int edt = (x_{des} - x) \tag{2.31}$$

then, the Equation (2.29) is reduced to

$$F_{des}^{r} = K_p e + K_i \int edt + bv \tag{2.32}$$

The Equation (2.32) can be discretized as follows.

$$A = \left(K_p + K_i \frac{T_S}{2}\right) \quad B = \left(-K_p + K_i \frac{T_S}{2}\right) \tag{2.33}$$

$$F_{des,k}^{r} = F_{k-1}^{r} + Ae_k + Be_{k-1} + bv_k \tag{2.34}$$

where, T_S is the sampling time, F_{k-1}^{r} is the force applied by the robot at time step *k-1*, which is measured by the force sensor at the wrist of the robot, and $e_k = \hat{v}_{k+1|k} - v_k$ (refer to Equation (2.28); $\hat{v}_{k+1|k}$ is already estimated in $\hat{\boldsymbol{x}}_{k+1|k}$).

During the task execution, the impedance damping, *b*, is adjusted by a fuzzy controller adaptively. We modify the damping coefficient of the impedance controller since controlling the velocity of the table is our primary goal. The damping coefficient is modified online by a fuzzy logic algorithm based on the estimated intentions of the human operator. This algorithm takes the current velocity of the table, v_k, and the rate of change of the human force estimated by the Kalman observer as the inputs, $\hat{F}_k^h$, and outputs a gain value representing the human intention, K_{HIG}, which is utilized to calculate the damping coefficient later.

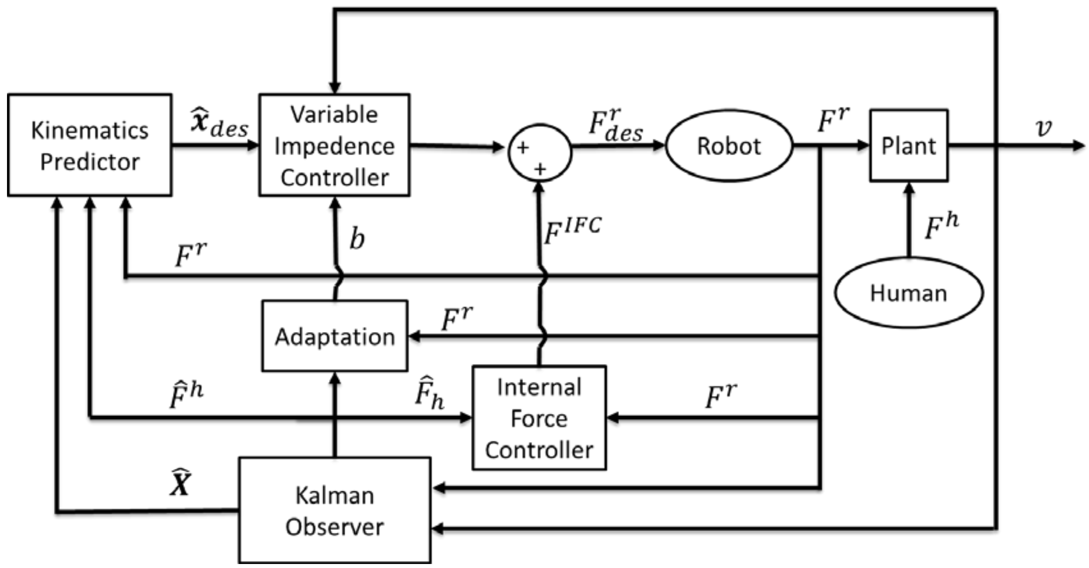

Figure 2.2. Control diagram of the table transportation task.

A fuzzy control system is based on fuzzy logic. Fuzzy logic has been used in many areas of intelligent control systems. Compared to traditional binary sets, fuzzy logic variables may have a truth value that ranges in degree between 0 and 1. In this sense, we can say binary logic is a special case of fuzzy logic. This feature enables us to define linguistic variables, such as very large, large, medium, small, very small, etc. Online parameter tuning is one of the important applications of fuzzy logic that is mostly used to update the parameters of the different types of controllers. Two-input-one-output Takagi-Sugeno fuzzy tuner is the most popular one and utilized in this study. In our case, the two inputs are velocity of the table and the derivative of the force applied by the human operator, and for each of them three membership functions (positive, zero and negative) are defined, as tabulated in Table 2.1. Using these two inputs (velocity of the table and the derivative of the force), we aim to infer the intentions of the human operator. If the velocity of the table is positive and the human force increases (i.e. derivative of the force is positive), we assume that the human operator desires to accelerate the table. If the human force decreases while the velocity is still positive, it is assumed that the human operator desires to decelerate the table. On the other hand, if the velocity is negative and the human force increases (decreases), then it is assumed that the human operator desires to decelerate (accelerate) the table. A similar approach, (without the fuzzy controller) is followed by Duchaine and Gosseline (2007) to adaptively adjust the damping coefficient of a variable impedance controller for a pHRI task.

Table 2.1: The singletons associated with the human intentions. The human intention gain for acceleration varies between $0 < \mathrm{K}_{\mathrm{HIG,k}} \leq 1$, the human intention gain for deceleration varies between $-1 \leq \mathrm{K}_{\mathrm{HIG,k}} < 0$, and $\mathrm{K}_{\mathrm{HIG,k}} = 0$ when there is no change.

$d\hat{F}_k^h$ \ v_k	Positive	Zero	Negative
Positive	1	0.5	-1
Zero	0	0	0
Negative	-1	-0.5	1

For the output, 5 singletons (-1, -0.5, 0, 0.5 and 1) are considered. Since there are three membership functions for each input, overall, we have nine (3x3) rules. To interpret these (i.e. inference mechanism), min-product method is used. Finally, center of gravity (COG) method is utilized to defuzzify the inferred fuzzy sets. This defuzzified value is, in fact, our human intention gain, $K_{HIG,k}$. For example, if $d\hat{F}_k^h > 0$ and $v_k > 0$, then the damping coefficient of the impedance controller is increased and hence the robot applies more force to the table in the desired direction. Note that if the derivative of the force applied by the human operator is zero, then, we assume that the human operator is happy with its current state, and we make no adjustment in the impedance of the robot.

The robot should comply with the human intentions in a pHRI task. In our approach, this is achieved by adjusting the damping coefficient of the impedance controller through the robot reaction gain, $K_{RRG,k}$. This gain takes a high or a low value depending on how fast the robot should react to the human intentions. For example, if the human intention is to accelerate the table, the velocity of the table is positive, and the force applied by the robot at the previous time step *k-1* is positive, then the robot already complies with the human intentions and hence the force applied by the robot at the current time step, k, does not require an immediate adjustment. As a result, the robot reaction gain, $K_{RRG,k}$ is set to a low value. On the other hand, if the human intention is to accelerate the table, the velocity of the table is positive, but the force applied by the robot at the previous time step *k-1* is negative, then there is a disagreement with the human intentions and hence the force applied by the robot at the current time step, k, requires an immediate adjustment. As a result, the robot reaction gain, $K_{RRG,k}$ is set to a high value.

We multiply the human intention gain, $K_{HIG,k}$ with the robot reaction gain, $K_{RRG,k}$ to calculate the damping coefficient of the impedance controller as

$$b_k = b_0 + K_{HIG,k} K_{RRG,k} \tag{2.35}$$

where, b_0 is the nominal value of the damping coefficient, which is constant and b_k is the variable damping coefficient at time instant k. Hence, the force applied by the robot takes the form of:

$$F_{des,k}^{r} = F_{k-1}^{r} + Ae_k + Be_{k-1} + b_k v_k \tag{2.36}$$

Table 2.2: The robot reaction to the human intention

Human Intention	v_k	F^r_{k-1}	$K_{RRG,k}$
Acceleration (+)	+	+	Low
Acceleration (+)	+	-	High
Acceleration (+)	-	+	High
Acceleration (+)	-	-	Low
Deceleration (-)	+	+	High
Deceleration (-)	+	-	Low
Deceleration (-)	-	+	Low
Deceleration (-)	-	-	High

So far, the proposed controller for the robot is designed to comply with the human intentions. However, due to time delays and/or noise in the system, conflicts may still occur. To reduce these conflicts, we utilize the internal force controller. This controller has been utilized successfully to manipulate an object using multiple robotic arms (Bonitz and Hsia, 1996). The goal in this approach is to decompose the forces applied by the robotic arms on the object into two components, namely motion-inducing and internal force, and then eliminate the internal force component. To our knowledge, this controller has not been utilized for pHRI though the "internal force" has been used as a measure of agreement/disagreement in some pHRI studies (Ikeura et al., 1994; Groten et al., 2009; Stefanov et al., 2009; Kucukyilmaz, 2013; Mörtl et al., 2012). In these studies, the net force acting on the object is calculated by adding the forces applied by the human operator and the robot as

$$F_{motion} = F^r + F^h \tag{2.37}$$

The forces applied by the human and the robot is decomposed into two components; one contributing to the motion of the object and the other is the internal force (i.e. wasted force), which does not contribute to the motion at all.

$$F^r = F^r_{motion} - F^{int} \tag{2.38}$$

$$F^h = F^h_{motion} + F^{int} \tag{2.39}$$

The internal force is defined as follows;

$$F^{int} = \begin{cases} F^h, & if\ (F^hF^r \leq 0) \wedge (|F^h| \leq |F^r|) \\ -F^r, & if\ (F^hF^r \leq 0) \wedge (|F^h| > |F^r|) \\ 0, & otherwise \end{cases} \tag{2.40}$$

In our case, the human operator is the leader and the robot is the follower. Also, the robot always complies with the human operator. Hence, when there is a disagreement between the human operator and the robot ($F^hF^r < 0$) due to time delays and/or noise in the system, we assume that the robot is the one responsible from the disagreement. Accordingly, the internal force in our approach is calculated as

$$F^{int} = \begin{cases} -F^r, & if\ (F^hF^r \leq 0) \\ 0, & otherwise \end{cases} \tag{2.41}$$

In order to eliminate this wasted force (i.e. internal force), a simple PI controller with a set value of zero is utilized.

$$F^{IFC} = k_p\left(0 - F^{int}\right) + k_i \int \left(0 - F^{int}\right) dt \tag{2.42}$$

where, k_p and k_i are the gains of the internal force controller.

In discrete domain, the above equation takes the form of

$$F_k^{IFC} = F_{k-1}^{IFC} - k_A F_k^{int} - k_B\, F_{k-1}^{int} \tag{2.43}$$

$$k_A = \left(k_p + k_i \frac{T_S}{2}\right) \quad k_B = \left(-k_p + k_i \frac{T_S}{2}\right) \tag{2.44}$$

Here, k_A and k_B are the discrete PI controller gains and F^{IFC} is the compensation signal that the PI controller generates to reduce the internal force between the human operator and the robot. Thus, the force that will be applied by the robot to the table becomes,

$$F_{des,k}^{r} = F_{k-1}^{r} + Ae_k + Be_{k-1} + b_k v_k + F_k^{IFC} \tag{2.45}$$

Chapter 3

SIMULATION

We have developed a simulation model in Matlab/Simulink environment to further investigate our approach. The main simulated scenario is relatively simple: human operator and the robot move the table starting from the origin and go to a station point and wait there for a while and then move backwards to a final destination point between the origin and the station. To implement this scenario, first, a desired trajectory profile is generated for the table based on the minimum jerk principle (Figure 3.1). Flash and Hogan (1985) suggested that smoothness of a motion can be quantified as a function of jerk, which is the time derivative of acceleration. Maeda et al. (2001) used the minimum jerk principle to estimate the desired trajectory of a long object that the human partner intends to manipulate with a robotic partner. Second, the minimum jerk trajectory is inputted to a simple PD controller to generate the “virtual” forces applied by the human operator to the table (In a real-life scenario, there is no need to generate a trajectory for the table since the human operator knows where to move the table). Third, the Kalman observer takes the output of the plant (velocity of the table) and the force applied by the robot to the table and estimates the force applied by the human operator. Fourth, the kinematics predictor utilizes this estimated force of the human operator, the force applied by the robot, the previous states of the table and the measured (current) velocity of the table to predict the upcoming states of the system. Finally, the impedance controller utilizes the estimated human force, predicted states of the next time step and the measured (current) velocity to generate the force applied by the robot to the table. Note that the impedance controller knows neither the reference trajectory in advance nor the measured force applied by the human operator.

In addition to the trajectory specified above, to further investigate the effect of internal force controller, another more complicated trajectory is generated and utilized in simulations (Figure 3.2).

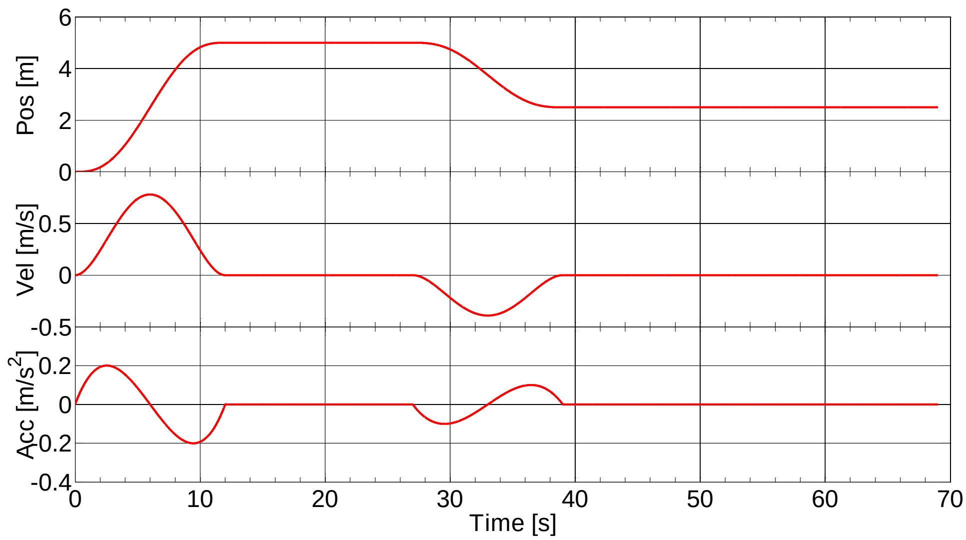

Figure 3.1. Scenario 1: The minimum jerk trajectory utilized in our Matlab/Simulink simulations.

During the simulations, three (3) controllers are tested in four (4) combinations:

SIC	: Standard Impedance Controller
VIC	: Variable Impedance Controller
SIC + IFC	: Standard Impedance Controller + Internal Force Controller
VIC + IFC	: Variable Impedance Controller + Internal Force Controller

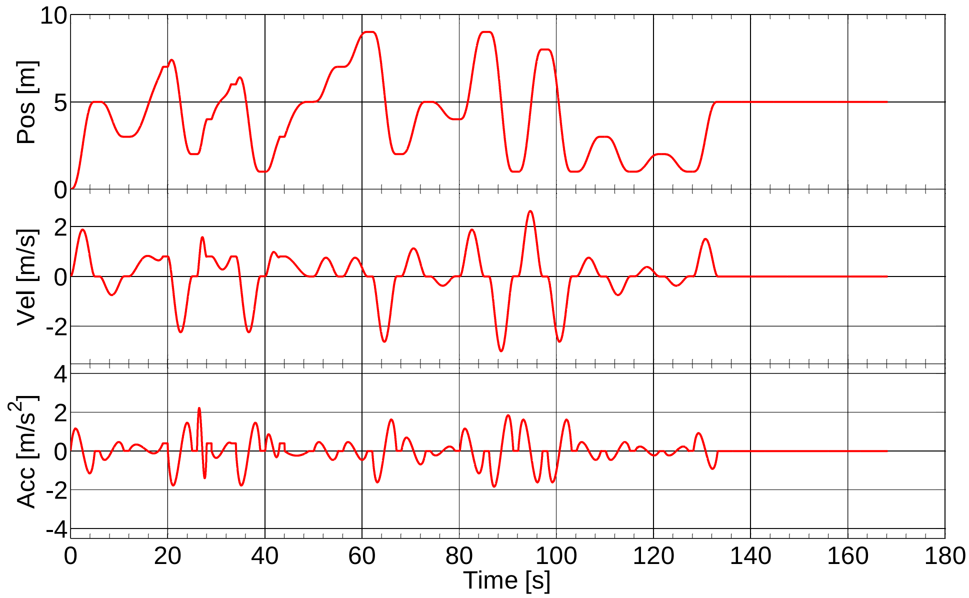

Figure 3.2. Scenario 2, that is utilized to further investigate the effect of IFC.

3.1 Performance Measures

We defined three measures to compare the performance of the proposed controllers. Our first measure is based on the tracking position error. We compare the tracking errors of the proposed controllers using two generic performance indices. One of them is the integral of square error (ISE) of position and the other is integral of time square error (ITSE) of position. ISE is a simple and time-independent index. However, ITSE is a time-dependent index and penalizes the positional errors made towards the end of task.

$$ISE = \int_0^{T_f} (x_{des} - x)^2 \, dt \tag{3.1}$$

$$ITSE = \int_0^{T_f} t(x_{des} - x)^2 \, dt \tag{3.2}$$

The second measure is based on the average force. To calculate the average force, we first calculate the impulse by integrating the force over time and then divide it by the task duration. We calculate the average force applied by a) the human operator and b) the robot, as well as c) the average internal force.

$$F^{r}_{ave} = \frac{\int_0^{T_f} |F^r| \, dt}{T_f} \tag{3.3}$$

$$F^{h}_{ave} = \frac{\int_0^{T_f} |F^h| \, dt}{T_f} \tag{3.4}$$

$$F^{int}_{ave} = \frac{\int_0^{T_f} \left|F^{int}\right| \, dt}{T_f} \tag{3.5}$$

Our last measure is based on the energy. We calculate and compare the effort made by the human operator and the robot (Kucukyilmaz et al., 2012). Note that T_f is the task duration in Equations (3.6) and (3.7). The efficiency of the cooperation is calculated in Equation (3.8).

$$E_r = \int_0^{T_f} |F^r . v| \, dt \tag{3.6}$$

$$E_h = \int_0^{T_f} |F^h . v| \, dt \tag{3.7}$$

$$Efficiency = \frac{\int_0^{T_f} |(F^r + F^h). v| \, dt}{\int_0^{T_f} |F^r . v| \, dt + \int_0^{T_f} |F^h . v| \, dt} \tag{3.8}$$

Chapter 4

RESULTS & DISCUSSION

Using the metrics defined in the previous section, we compare the performance of the proposed controllers (SIC, VIC, SIC + IFC, VIC + IFC).

In terms of tracking performance, we easily observe that the overshoot amplitudes are higher under SIC compared to that of VIC (see Figure 4.1). Hence, the positional errors under SIC are significantly higher than that of VIC (see Figure 4.2). IFC also contributes to the reduction of ISE and ITSE, but its contribution to VIC is small (see Figure 4.2). However, among the 4 controllers, the performance of VIC+IFC is the best in terms of ITSE.

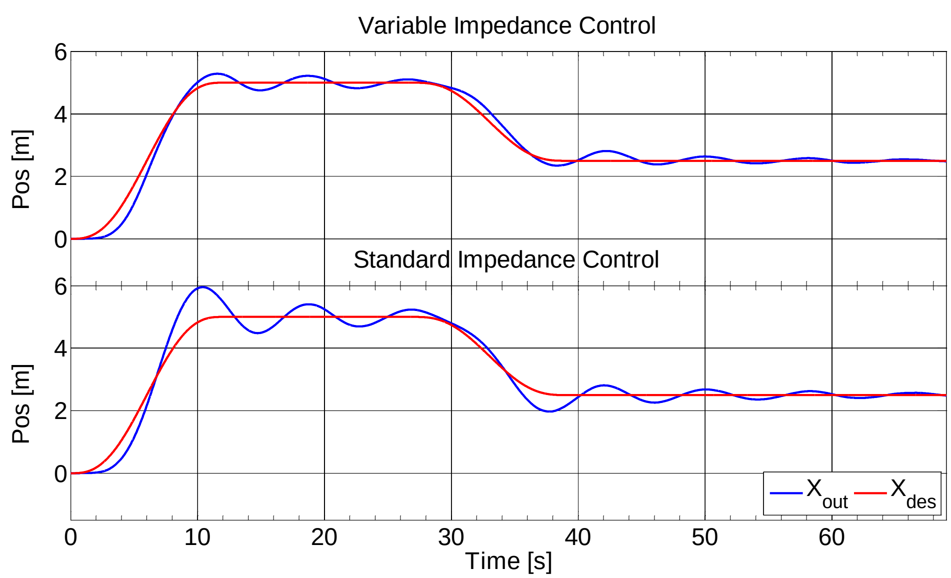

Figure 4.1. The position tracking performance of VIC and SIC.

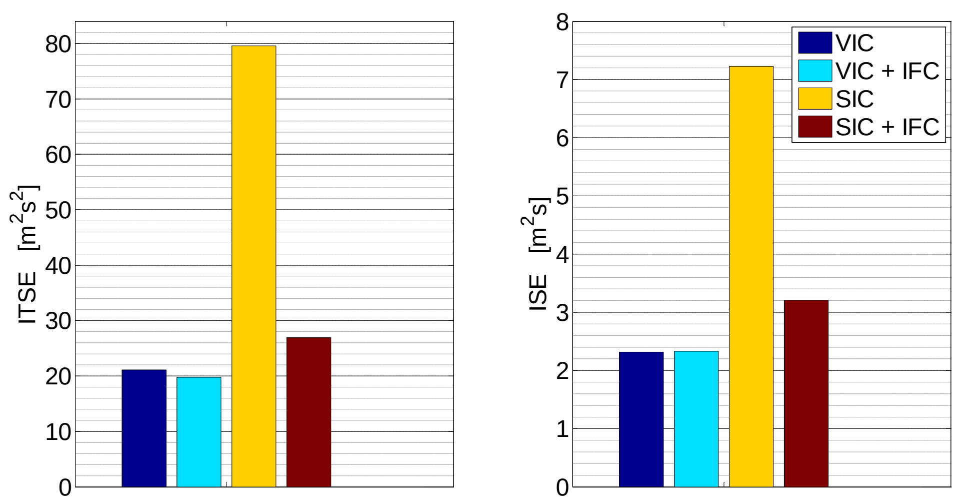

Figure 4.2. The comparison of the proposed controllers based on ITSE and ISE indices.

In terms of the average force, as shown in Figure 4.3, the average forces of both the human operator and the robot are reduced under VIC compared to SIC. Also, SIC+IFC reduces the average forces applied by the partners on the table when compared to using SIC alone. However, as it is observed from the Figure 4.3, there is not much change in the average forces of the human operator and the robot when the controller is changed from the VIC to VIC+IFC.

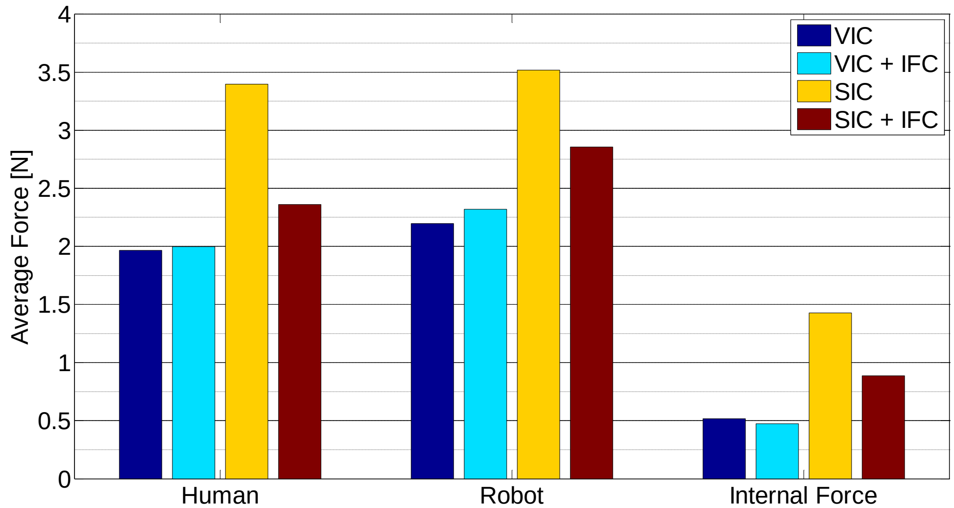

Figure 4.3. The average force applied by the human operator and the robot on the table and the average internal force.

The average internal force for different controllers is shown in Figure 4.3. The amount of disagreement between the human operator and the robot is the highest under SIC. IFC reduces the disagreement to some extent. Moreover, VIC further reduces the disagreement and the least disagreement between the collaborating partners is observed under VIC+IFC.

The main reason why the average forces applied by the collaborating partners are reduced significantly under VIC is the impedance adaptation mechanism based on human intention estimation. In VIC, since the human intention is estimated at each time step during the task execution, the partners are in agreement most of the time and contribute to the task in a desired manner.

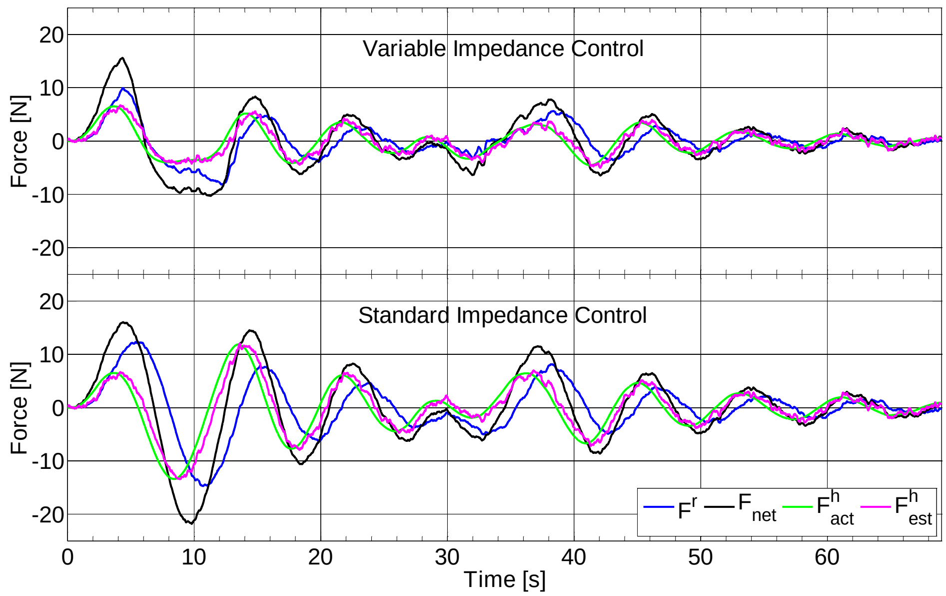

Figure 4.4. The force profiles of the human operator and the robot under VIC and SIC.

Figure 4.4 shows the force profiles of the human operator and the robot under VIC and SIC. One can observe from Figure 4.4 that the forces applied by the robot to the table under SIC are delayed, resulting in more force conflicts between the collaborating partners (see Figure 4.3). During the task execution, the forces applied by the human operator show some variation due to change in his/her intentions. Although the Kalman observer estimates the force applied by the human operator at each time step during the task, SIC cannot compensate for the variations in this force. Since the robot adjusts its impedance based on the human intention and alters its force adaptively under VIC, there is less disagreement between the partners. This is easily observed from the internal force plots in Figure 4.3; the average internal force (a measure of disagreement) under VIC is significantly less than that of SIC. Moreover, one can also observe that the addition of IFC further reduces the disagreements (conflicts) between the collaborating partners.

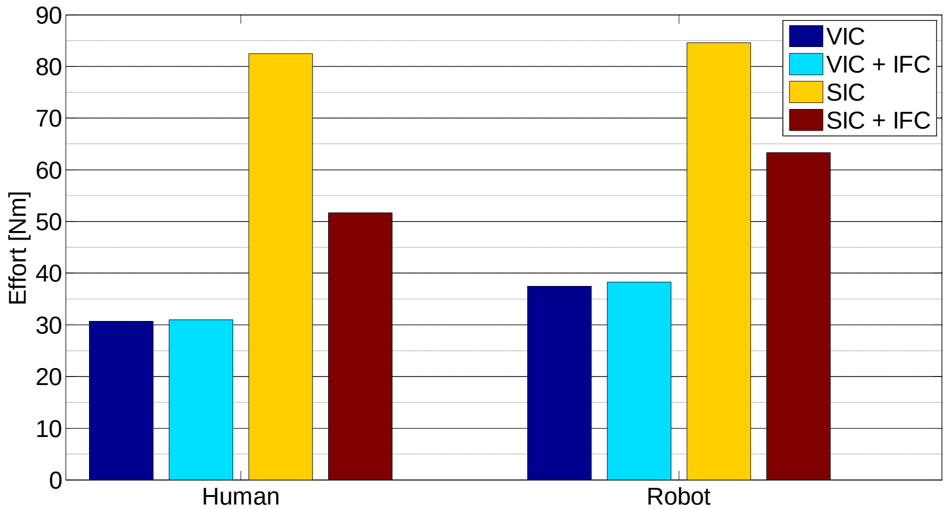

Figure 4.5. The efforts made by the human operator and the robot.

In terms of the effort made by the collaborating partners to execute the task, we observe that the energies spent by the human operator and the robot are highest under SIC (see Figure 4.5). The addition of IFC to SIC (i.e. SIC+IFC) reduces the energy spent by the partners to execute the task, but using VIC leads to much higher reduction. On the other hand, the addition of IFC to VIC (i.e. VIC+IFC) slightly increases the effort made by the human operator and the robot. In Figure 4.6a, we plot the ratio of the efforts to observe the relative contribution of the robot to the task with respect to the human operator. Here, we observe that the relative effort made by the human operator is the lowest under VIC+IFC. Hence, although the individual efforts of the human operator and the robot increases slightly under VIC+IFC compared to VIC (see Figure 4.5), the human operator performs less work compared to the robot under VIC+IFC (see Figure 4.6a). The efficiency plot shown in Figure 4.6b also supports this claim. Among the four controllers proposed in this study, VIC+IFC scheme has the highest task efficiency.

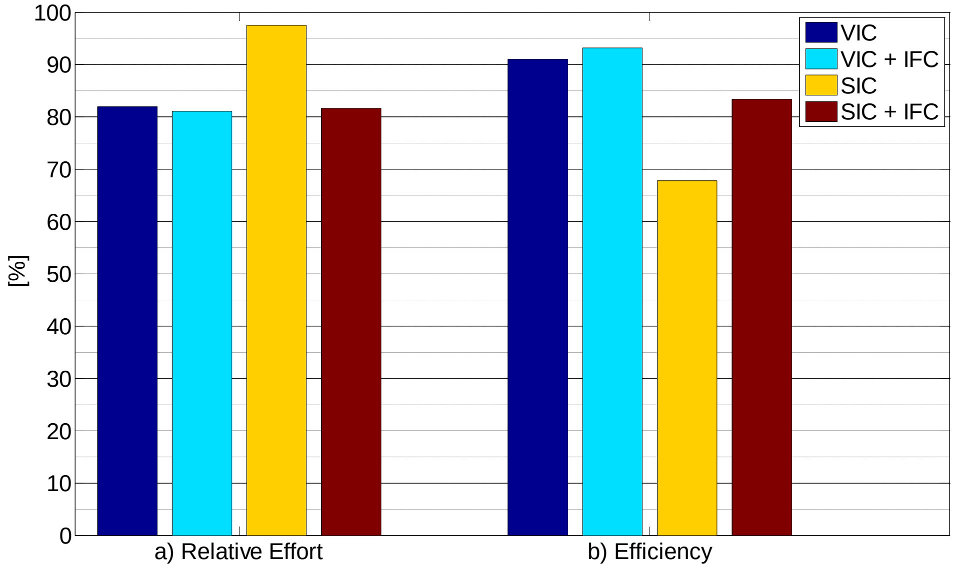

Figure 4.6. a) The relative effort of the human operator with respect to the effort of the robot. b) The efficiencies of the proposed controllers.

Up to now, VIC seems to perform better than SIC and SIC+IFC. However, to show contributions of IFC with VIC+IFC is needed to be expressed. To show the contributions of IFC to VIC, average internal force of the main scenario (for scenario 1, see Figure 3.1) and the second scenario (for scenario 2, see Figure 3.2) are compared in Figure 4.7. As the task gets more complex, it is obvious that the conflict between the robot and the human operator tends to increase. VIC reduced the internal force significantly in both scenarios. However, since the conflicts are much higher in the second scenario, VIC itself cannot handle these conflicts by itself alone as efficiently as the previous scenario. It is obvious from the actual and normalized values of internal force (see Figure 4.7), as the task gets more complicated, the contribution of IFC in the reduction of internal forces become more significant under VIC+IFC.

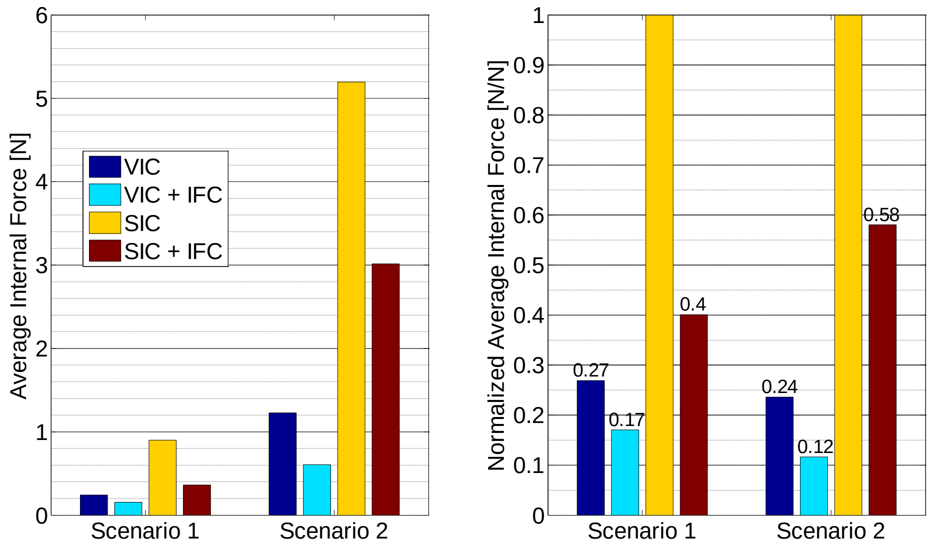

Figure 4.7. Average internal force comparison of two scenarios.

Chapter 5

CONCLUSION

We aim to develop a controller for a robot that can intuitively understand the intentions of a human partner and collaborates with him/her naturally and efficiently during a pHRI task. In order to achieve this goal, we have developed a variable impedance controller and compared its performance with a conventional (standard) impedance controller. We modify the damping coefficient of the variable impedance controller on the fly to comply with the intentions of the human operator during the task execution. This modification is achieved through a fuzzy controller, which utilizes the derivative of the force applied by the human (estimated via a Kalman observer) and the velocity of the object being manipulated to estimate the intention of the human operator. The robot should react to changes in the human intention immediately in order to reduce the conflicts. In our approach, the level of human intention and the scale of the robot’s reaction to this intention set the magnitude of the damping coefficient of the variable impedance controller.

Although the performance of the proposed variable impedance controller is better than that of the standard impedance controller, the delays and uncertainties in the system may still cause some conflicts between the human operator and the robot. As a remedy to this problem, we utilize an internal force controller in series with the variable impedance controller. Although this scheme (VIC + IFC) increases the total effort made by the collaborating partners slightly, it further reduces the conflicts and improves the task efficiency.

Chapter 6

FUTURE WORK

The results presented in this thesis are based on 1D simulations performed in Matlab/Simulink environment. In our scenario, the collaborating partners moved a point mass back and forth along a straight path. We have chosen this relatively simple scenario to better understand the nature of the interactions taking place between the collaborating partners and to diagnose the implementation problems more easily. The next step is to perform rigid body simulations in 2D (i.e. planar motions). Although implementing rigid body dynamics in 2D is trivial, the inclusion of the rotational motion will bring additional challenges and require more effort for detecting the intention of the human operator and resolving the ambiguities. For example, consider the following scenario shown in Figure 6.1. The human operator applies a force to the table along the y-axis (Figure 6.1a), but his/her intention is not clear; does he/she intend to translate the table along the y-axis (Figure 6.1b) or rotate it about the z-axis (perpendicular to the xy plane)? In order to resolve the ambiguity stated above, we need to better understand the haptic interactions taking places between two collaborating human partners. For this reason, we plan to conduct experiments with human dyads in virtual environments using haptic devices. In our experiments, the collaborating partners will transport a table on a plane and feel the interaction forces through their haptic devices. With the knowledge and experience gained from these experiments, we plan to further improve the approach proposed in this thesis.

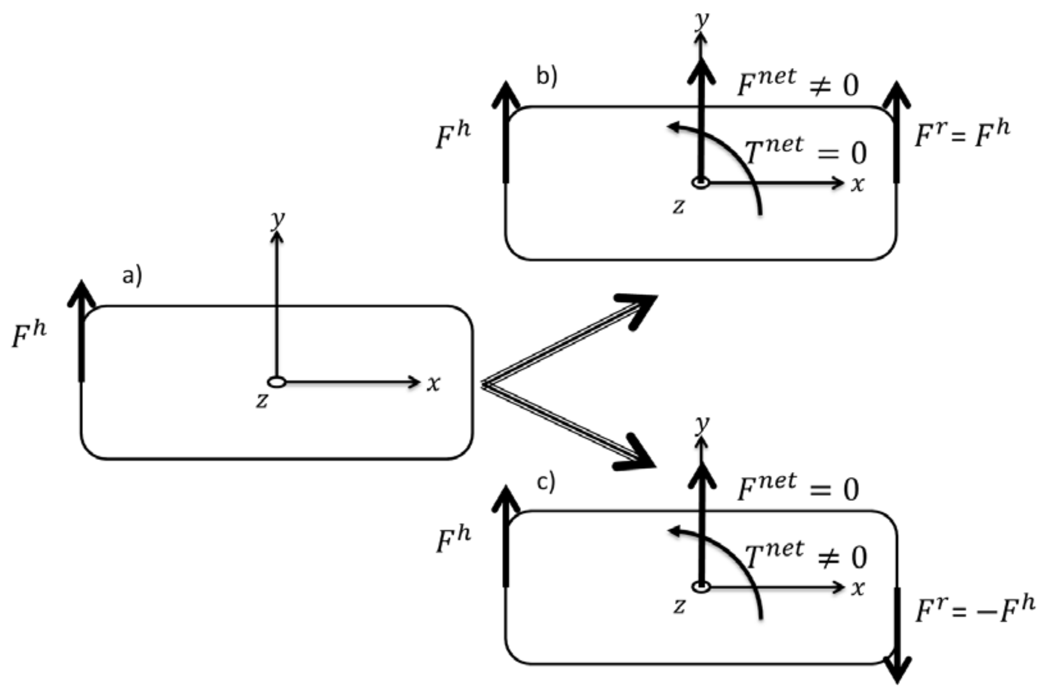

Figure 6.1. Ambiguity in detecting human intention during the table transportation task performed in 2D; a) Human applies a force in y-direction, b) the robot assumes that human intends to translate along the y-axis, c) the robot assumes that human intends to rotate about the z-axis.

BIBLIOGRAPHY

Bonitz , R., G., and Hsia, T., C., (1996) “Robust internal-force based impedance control for coordinating manipulators—Theory and experiments,” in Proc. IEEE Int. Conf. Robotics Automation, 1996, pp. 622–628.

de Carli,D.,Hohert, E., Parker, C. A. C., Zoghbi, S., Leonard, S., Croft, E. and Bicchi, A.(2009). "Measuring Intent in Human - Robot Cooperative Manipulation". IEEE International Workshop onHaptic Audio Visual Environments andGames, pp: 6.

Dourish, P. and Bellotti, V. (1992). Awareness and coordination in shared workspaces. In Proceedings of the 1992 ACM conference on Computer-supported cooperative work, CSCW ’92, pages 107–114, New York, NY, USA. ACM.

Duchaine, V. and Gosselin, C. M. (2007). General model of human-robot cooperationusing a novel velocity based variable impedance control. InWHC’07: World Haptics Conference, pages 446–451.

Dumora, J., Geffard, F., Bidard, C., and Fraisse, P. (2013). Towards a robotic partner for collaborative manipulation. In HRI Workshop on Collaborative Manipulation.

Flash, T. and Hogan, N. (1985). The coordination of arm movements: An experimentally confirmed mathematical model. J. Neurosci., 5:1688–1703.

Groten R, Feth D, Goshy H, Peer A, Kenny D and Buss M (2009). Experimental analysis of dominance in haptic collaboration. In Proceedings IEEE RO-MAN, pp. 723–729.

Hogan, N. (1985) Impedance Control: An Approach to Manipulation. Part I: Theory, ASME Journal of Dynamic Systems Measurement and Control, Vol. 107, pp. 1-7.

Ikeura R, Monden H and Inooka H (1994) Cooperative motion control of a robot and a human. In Proceedings IEEE RO-MAN, pp. 112–117.

Ikeura R, Moriguchi T and Mizutani K (2002) Optimal variable impedance control for a robot and its application to lifting an object with a human. In Proceedings IEEE RO-MAN, pp. 500–505.

Jung, S., Hsia, T. C., and Bonitz, R. G. (2004). Force tracking impedance control of robot manipulators under unknown environment. IEEE Transactions on Control Systems Technology 12, 3, 474–483.

Maeda, Y., Hara, T., and Arai, T. (2001). Human-Robot Cooperative Manipulation without Motion Estimation. In Proc. IEEE/RSJ IROS, pages 2240–2245

Kucukyilmaz, A., Sezgin, T. M., and Basdogan, C. (2013). Intention recognition for dynamic role exchange in haptic collaboration. IEEE Transactions on Haptics, 6(1):58–68.

Moertl, A., Lawitzky, M., Kucukyilmaz, A., Sezgin, T. M., Basdogan, C., and Hirche, S. (2012). The role of roles: Physical cooperation between humans and robots. Int. J. Rob. Res., 31(13):1656–1674.

Oguz, S.O., Kucukyilmaz, A., Sezgin, T.M., Basdogan, C., 2010, “Haptic Negotiation and Role Exchange for Collaboration in Virtual Environments”, Proceedings of IEEE Symposium on Haptics, March 25-26, Waltham, MA, pp. 371-378.

Seraji, H., and Colbaugh, R. (1997). Force tracking in impedanc control. International Journal of Robotics Research 16, 1, 97–117.

Stanisic, R. Z., and Fernandez, A. V. (2012). Adjusting the parameters of the mechanical impedance for velocity, impact and force control. Robotica 30, 583–597.

Stefanov, N., Peer, A., and Buss, M. (2009). Role determination in human-human interaction. In WHC’09: World Haptics Conference, pages 51–56, Washington, DC, USA. IEEE Computer Society.

Takubo T, Arai H, Hayashibara Y and Tanie K (2002) Human–robot cooperative manipulation using a virtual nonholonomic constraint. The International Journal of Robotics Research 21: 541–553.

Wojtara, T., Uchihara, M., Murayama, H., Shimoda, S., Sakai, S., Fujimoto, H., and Kimura, H. (2009). Human-robot collaboration in precise positioning of a threedimensional object. Automatica, 45:333–342.